Int J Multiphase Flow Vol 12, No 4, pp 609–625, 1986
Printed in Great Britain

0301-9322/86 $3.00+.00
Pergamon Journals/Elsevier

TWO-PHASE FLOW THROUGH SMALL BRANCHES IN A HORIZONTAL PIPE WITH STRATIFIED FLOW

C. SMOGLIE
Centro Atomico, 8400 Bariloche, Argentina

and

J. REIMANN
Kernforschungszentrum Karlsruhe, Institut für Reaktorbauelemente, Postfach 3640, 7500 Karlsruhe 1, Federal Republic of Germany

Abstract—Accurate prediction of the mass flux and quality through small breaks in a horizontal coolant pipe, where stratified flow exists, is of great importance in nuclear reactor safety research. Experiments were performed with air–water flows through breaks simulated by pipe stubs of various diameters located at the bottom, the top or in the side of a horizontal pipe. The flow phenomena observed are illustrated with photographs. Correlations are given for the beginning of entrainment. Measurements were made of the entrainment beginning of the break quality and mass flux for different values of the interface level, and of the pressure difference between main pipe and break outlet. A model was developed to predict the branch quality and mass flux. This model can also be applied to steam–water critical branch mass flux, as is shown in an example.

1. INTRODUCTION

The two-phase flow through T-junctions has gained increasing interest in the past few years. In view of the technical applications in piping networks of chemical plants and power plants, investigations were concentrated on flow and geometrical parameters quite different from those applying to situations of interest in nuclear reactor safety, i.e. loss of coolant accidents (LOCA) caused by small breaks in horizontal coolant pipes. During such a LOCA, a stratified flow may occur in the horizontal pipe, which severely influences the mass flow rate through the break. Breaks are usually simulated by T-junctions with a small ratio d/D of branch to main pipe diameter. Contributions related to this problem were made by Henry (1981), Azzopardi & Whalley (1982), Saba & Lahey (1984), and Seeger *et al.* (1985).

Zuber (1981) pointed out that the information available on these processes did not correspond to conditions of interest in nuclear reactors (figure 1). If a break is located above the horizontal interface, liquid from the interface can be entrained due to the pressure drop at the interface produced by the vapor acceleration in the vicinity of the break (Bernoulli effect). Similarly, with a break located below the interface, vapor can reach the break due to vortex formation or can be pulled through in a vortex-free flow. Flow conditions are characterized by: (a) flow geometry without axial symmetry, (b) the existence of a remaining flow rate downstream of the break, which will be termed "superimposed velocity" to indicate that there is a net fluid velocity perpendicular to the break flow.

Investigations on this subject were performed, for instance, by Dagget & Keulegan (1974), Lubin & Hurwitz (1966), Rouse *et al.* (1956), etc. However, those publications concentrate on the beginning of entrainment for other geometrical conditions and give no results for the quality and mass flux through the break.

Zuber stated that thermal hydraulic computer codes used currently, cannot predict satisfactorily either the beginning of entrainment or the amount of liquid or gas entrainment.

Considering Zuber's statements, several investigations were carried out: Crowley & Rothe (1981) performed some air–water experiments at a system pressure of 0.3 MPa in a horizontal pipe (D = 0.067 m) with a symmetrical afflux towards a side orifice (d = 0.006 m). Reimann & Khan (1983) investigated the air–water flow through downward oriented branches for various flow conditions in a horizontal pipe. The same facilities were used to perform experiments with upward branches (Reimann & Smoglie 1983) and horizontal branches (Smoglie & Reimann 1984). This article summarizes results described in detail by Smoglie (1984).

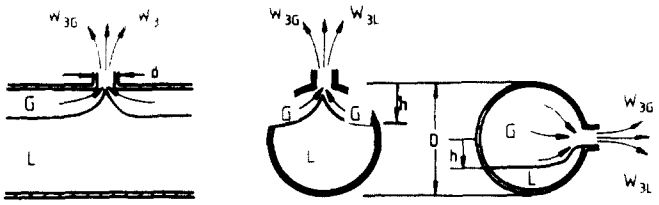

Liquid entrainment due to Bernoulli effect

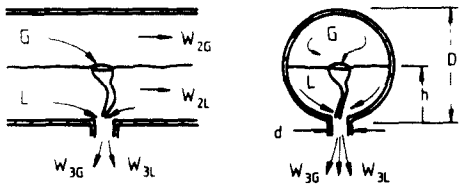

Gas entrainment due to vortex formation.

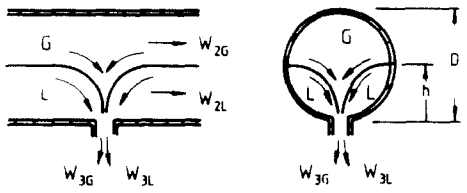

Gas entrainment in vortex free flow.

Figure 1 Mechanisms for liquid and gas entrainment in small breaks (Zuber 1981)

2 TEST FACILITY AND EXPERIMENTAL METHOD

Figure 2 shows a scheme of the air–water loop (for details see John & Reimann 1979). The air is supplied to the loop by a compressor followed by an air cooler, an air filter, a spring tube manometer and a mercury thermometer. Cold water is supplied from a reservoir with a circulating pump. At a maximal system pressure of 11 bar, maximal air and water mass flow rates of 1 kg/s and 30 kg/s respectively are provided. Branches with different diameters and orientations, perpendicular to the test section, are followed by throttle valves and can be connected to a separator for measurements of gas and liquid mass flow rates. Downstream of the test section, the air–water mixture is carried into a cyclone and, subsequently, the water is returned to the reservoir feeding the pump. Exchangeable orifices are used for measurements of single phase mass flow rates.

Figure 3 shows details of the test section. The inlet, run, and branch variables (W = mass flow rate, v = phase velocity) are characterized by the indices 1, 2, and 3, respectively. The main pipe (inner diameter D = 0.206 m, total length 6 m) includes an inlet chamber, designed to favor stratified flow, and a plexiglass pipe piece which contains exchangeable inserts for the different branches and allows the visual observation of the flow phenomena in the vicinity of the branch entrance. The branches (inner diameter d = 0.006, 0.008, 0.012 or 0.020 m) are pipe stubs with sharp-edged entrance length of 0.055 m and pressure taps at different positions along the branch axis.

The end of the test section can be removed (at A-A in figure 3) and closed by a flange containing a window for observation of the flow field in the direction of the pipe axis. At the test section exit, a special homogenizer is used to prevent pressure oscillations when a slug-type two-phase flow is throttled to atmospheric pressure. The system pressure P_1 is measured with an absolute pressure transducer about 0.5 m upstream of the T-junction.

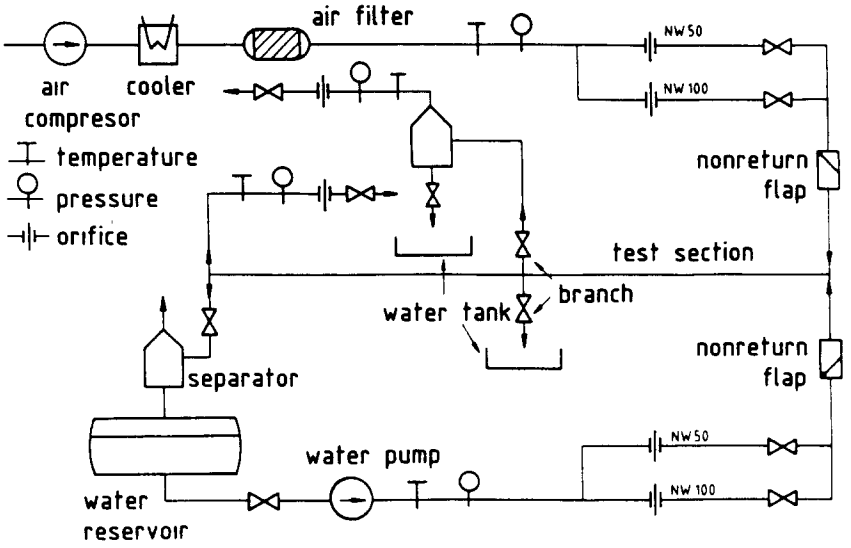

Figure 2. Two-phase flow air–water loop.

Differential pressure transducers are used for measurements of the liquid level h_L and the pressure differential ΔP_{1-3} between main pipe and branch; h_L can also be read from a vertical scale downstream of the branch in the plexiglass section.

The experiments were performed with stratified cocurrent air–water flow in the horizontal main pipe at ambient temperature and at a system pressure of 0.5 MPa for most of the experiments. ΔP_{1-3} was varied between 0.01 and 0.4 MPa by means of the throttle value downstream of the branch. Most of the experiments were performed with subcritical branch flow.

To determine the beginning of gas entrainment (b.g.e.) in downward and horizontal branches, either h_L was kept constant and ΔP_{1-3} was gradually increased, or the main pipe and branch mass flow rates were adjusted so that a very slowly decreasing liquid level occurred (for instance $\Delta h_L = 0.005$ m in 100 sec), at a constant system pressure (quasi steady-state experiments). The formation of the first gas tubes reaching the branch entrance produced a characteristic change in the signal of the ΔP_{1-3} transducer, which was considered as the b.g.e. In experiments with a superimposed liquid velocity, v_{2L} was calculated from the difference $W_{2L} = W_{1L} - W_{3L}$. For measurements of gas entrainment (g.e.), the valves at the exit of the test section were closed and a balance between the input and branch mass

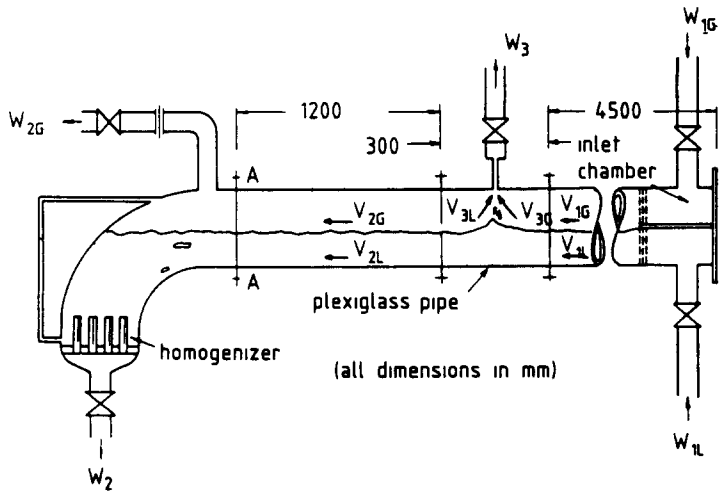

Figure 3 Test section

flow rates was adjusted so that P_1 and h_L were kept constant. Therefore, W_{3G} and W_{3L} were determined with the orifices preceding the main pipe inlet.

To determine the beginning of liquid entrainment (b.l.e.) in upward and horizontal branches, either h_L was kept constant and ΔP_{1-3} was increased gradually or a constant W_{3G} at a constant P_1 was adjusted to a slowly increasing liquid level (for instance, $\Delta h_L = 0.002$ m in 100 s). The b.l.e was determined visually and from the signals of the ΔP_{1-3} transducer when a few droplets raised from the interface reached the break outlet. In experiments with superimposed gas velocity, v_{2G} was calculated from the difference $W_{2G} = W_{1G} - W_{3G}$.

In order to measure the liquid entrainment (l.e.) we waited for the equilibrium between inflow and branch flow, then W_{3G} and W_{3L} were given by the measurements at the main pipe inlet. In experiments with upward branches, a small quantity of entrained liquid is mixed with a relatively high gas mass flow rate For mass flow measurements the branch was therefore connected to a separator

3 FLOW PHENOMENA

3.1 Downward branch

For an inflow rate equal to the branch flow rate, no resultant liquid flow perpendicular to the branch axis exists. This situation is highly unstable with an enhancement of velocity components circumferential to the branch axis, and therefore results in a vortex flow. Gas entrainment starts when a very thin gas tube reaches the branch inlet. This first gas tube is not stable but is swept away after some seconds and a long time can pass until another gas tube is formed. As the distance h from the branch entrance to the interface is shortened or W_{3L} is increased (higher ΔP_{1-3}), the gas tube becomes thicker and more stable (figure 4).

When the distance h to the interface is reduced further, a condition is reached where the flow pattern switches over from a vortex flow to a vortex-free flow. One reason for this transition is the increasing influence of the wall friction with decreasing interface levels.

Another transition from vortex to vortex-free flow occurs when the superimposed liquid velocity v_{2L} exceeds a certain value. For $v_{2L} \leqslant 0.06$ m/s the vortices are very unstable and for higher values the flow field observed in the experiments was always vortex free as shown in figure 5. In the photograph 5a the interface is already deflected considerably but gas entrainment does not yet occur. At a lowered interface level h (increased W_{3L}), the tip of the funnel-shaped interface begins to oscillate and gas is intermittently sucked into the branch (figure 5b). When the interface level is lowered still further, a continuous gas entrainment occurs (figure 5c)

3.2 Upward branch

For sufficiently large distance h between branch entrance and interface, only gas enters the branch, the interface being a nearly ideal horizontal plane. For smaller h, however, the interface below the branch entrance is locally raised due to the pressure drop in the gas flow towards the branch.

Figure 6 shows sequences of photographs taken from the end of the horizontal pipe for a further decreased distance h: a considerable amount of liquid can be torn away from the interface. However, the gas flow has a distinct vorticity which accelerates the droplets in the radial direction so that only a small portion of them reaches the branch inlet. The droplets hit the wall and give rise to a liquid film, most of which runs off due to gravity; only a small fraction near the inlet is sucked into the branch.

At high inlet gas fluxes ($v_{1G} \simeq 2$ m/s) surface waves occur which disturb the entrainment process and slightly reduce the amount of liquid entrained. Further increase in the input gas flow rate finally causes the transition from stratified to slug flow; the time-averaged branch liquid flow rate is then considerably increased.

The superimposed gas velocities ($v_{2G} < 2$ m/s) resulted in a slight displacement of the vortex axis and therefore of the deflected interface in the direction of the outflow. No effect

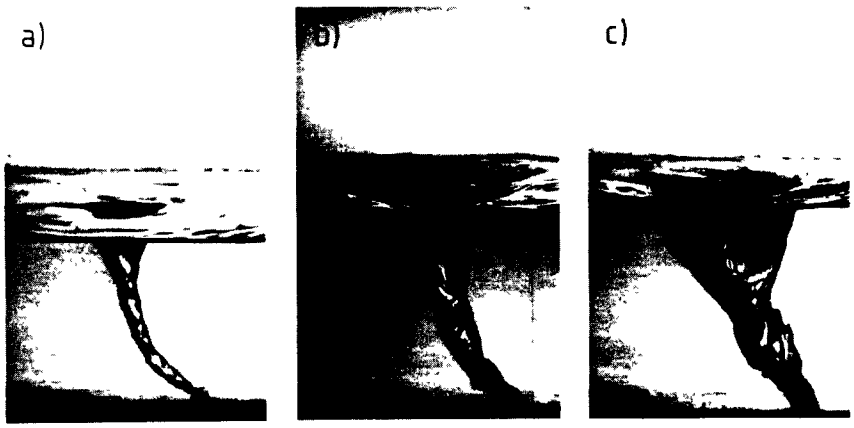

Figure 4 Vortex gas entrainment in downward branch, $v_{2L} = 0$ and increasing ΔP_{1-3} from (a) to (c)

of the superimposed liquid velocities on the position of the deflected interface was observed in the range investigated ($v_{2L} \leqslant 0.15$ m/s).

3.3 Horizontal branch

With the interface below the branch axis, the Bernoulli effect is evidenced first by the deflection of the interface in the vicinity of the pipe wall below the branch entrance. With further decreasing of the distance h between branch axis and interface, a thin rising film of water, not influenced by vorticity, determines the b.l.e. A superimposed gas velocity

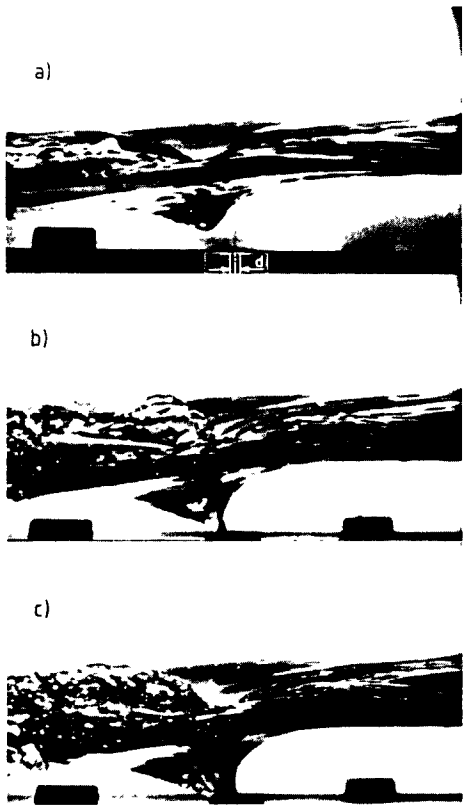

Figure 5 Development of vortex free gas entrainment in downward branch, $v_{2L} = 0.3$ m/s and increasing ΔP_{1-3} from (a) to (c)

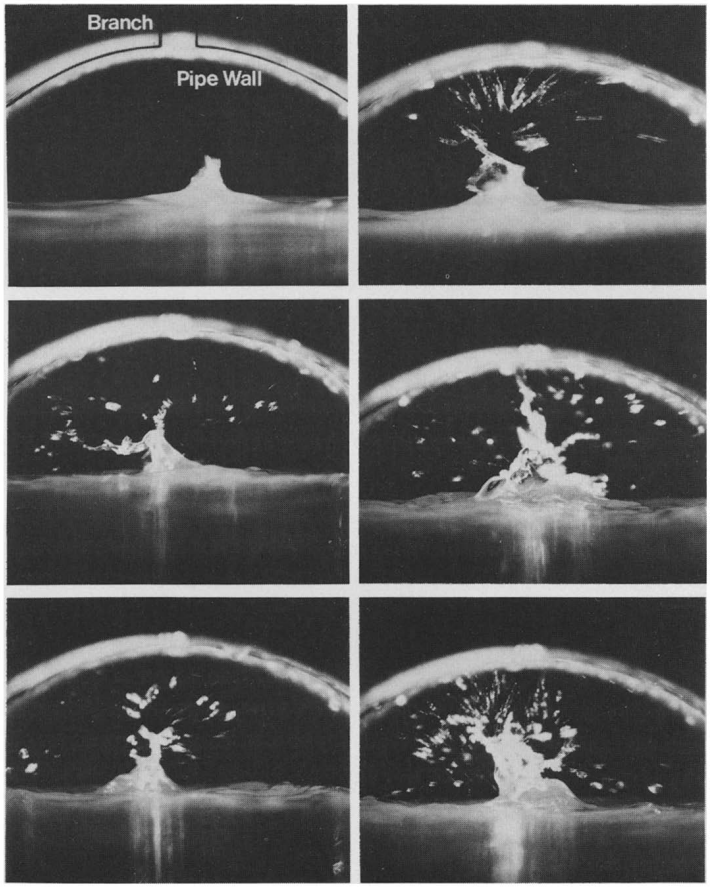

Figure 6 Liquid entrainment in upward branch (axial view)

causes no appreciable displacement of this water film because the friction forces dominate at the wall. Again, no essential influence of the superimposed liquid velocities on the rising liquid film is observed.

Figure 7 shows photographs of liquid entrainment, taken in the direction of the pipe axis, for a constant h and an increasing pressure difference ΔP_{1-3}. In figure 7a, a thin rising liquid film is seen whereas, at higher pressure differences (figures 7b and 7c), the liquid is dispersed into very small droplets due to the strong acceleration near the branch entrance.

With the liquid level located above the branch axis, the continuous liquid phase exhibits

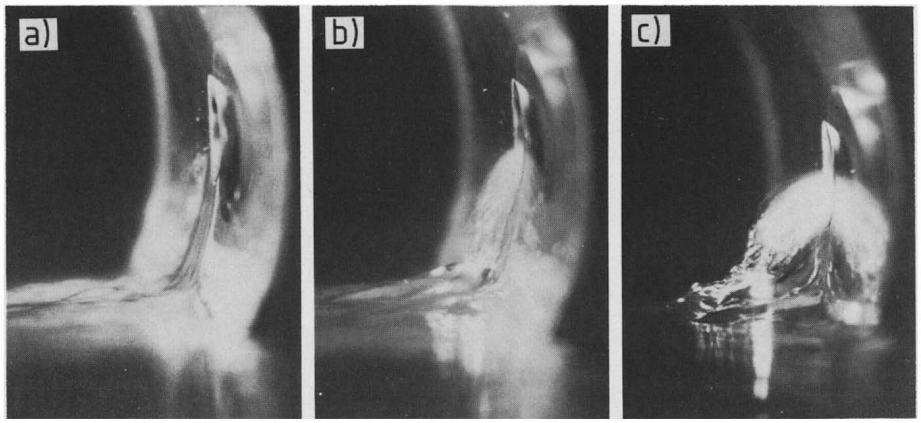

Figure 7 Liquid entrainment in horizontal branch (axial view) Increasing ΔP_1 from (a) to (c)

a very small vorticity difficult to observe on the interface. Along the vortex axis, at a short distance from the pipe wall, thin tubes of gas reach the branch entrance and determine the b.g.e. When the pressure difference is increased, the initial gas tubes are observed to rapidly approach the pipe wall. Wall friction prevents vorticity from developing and after short intermittencies the gas is in direct contact with the wall. Thus, the vorticity is completely suppressed and a vortex-free gas flow exists between the liquid and the pipe wall.

4 BEGINNING OF GAS AND LIQUID ENTRAINMENT

To describe the beginning of entrainment (b.e.) the effects of viscosity and surface tension were neglected and the symbols ρ_b and v_{3b} were respectively used for the density and the velocity of the continuous phase at b.e. Thus, at b.g.e.: $\rho_b = \rho_L$; $v_{3b} = v_{3L}$; and at b.l.e.: $\rho_b = \rho_G$; $v_{3b} = v_{3G}$.

By combination of these variables, the following dimensionless groups are proposed:

$$\frac{h_b}{d}, \mathrm{Fr} = \frac{\rho_b v_{3b}^2 b}{gd(\rho_L - \rho_G)}, \frac{\rho_G v_{2G}^2}{\rho_b v_{3b}^2}, \frac{\rho_L v_{2L}^2}{\rho_b v_{3b}^2}, \frac{d}{D}$$

The first group is the most important geometrical parameter since it represents the influence of the break size on the b.e.; the second group is the product of v_{3b}^2/gd and $\rho_b/(\rho_L - \rho_G)$ and represents the Froude Number (ratio of inertial to gravitational forces in the branch flow), the following two terms are ratios between momentum fluxes and constitute a relative magnitude of the superimposed velocities; the last group is a geometrical parameter indicating the relative size of the break.

In the range of the experiments, the momentum flux in the outflow was at least three orders of magnitude lower than the momentum flux in the branch. Therefore, no significant influence on the b.e. is expected of the superimposed velocities, and the groups containing v_{2G} or v_{2L} may be discarded.

For the investigated branches the ratio d/D was always smaller than 0.1 which means that a geometrical similitude can be assumed for the various flow fields, i.e. the b.e. can be considered independent of d/D. Therefore, only the correlation between h_b/d and the Froude number has to be investigated:

$$\left| \frac{v_{3b}^2 \rho_b}{gd\ (\rho_L - \rho_G)} \right|^a = K^* \frac{h_b}{d} \qquad [1]$$

where a and K^* are constants to be determined from the experiments.

Lubin & Hurwitz (1966) found the value of $a = 0.2$ for the b.g.e. in an initially stationary liquid draining through a circular orifice at the bottom of a cylindrical tank. The same value $a = 0.2$ was used by Reimann & Khan (1983) to describe the b.g.e. and the transition from vortex to vortex free flow in downward branches. The authors concluded that for $d/D << 1$ the flow field generated by the branch is equivalent to that due to a point sink at the branch entrance, i.e. it is dominated by the branch mass flow rate, not by the branch diameter. Therefore they proposed to substitute v_{3b} in the Froude number by $W_{3b}/\rho_b\ \pi\ d^2/4$ to obtain a correlation which does not depend explicitly on d:

$$\frac{h_b |g \rho_b (\rho_L - \rho_G)|^{0.2}}{W_{3b}^{0.4}} = K \qquad [2]$$

This equivalence with a point sink was also used by Craya (1949), who described analytically the b.l.e. in a side orifice above the interface between two liquids of different densities, with a correlation like [2], which was experimentally confirmed by Garnel (1949).

The same result was obtained assuming a point sink at the entrance of an upward branch and using the potential flow theory to determine the conditions for the b.l.e. (Smoglie

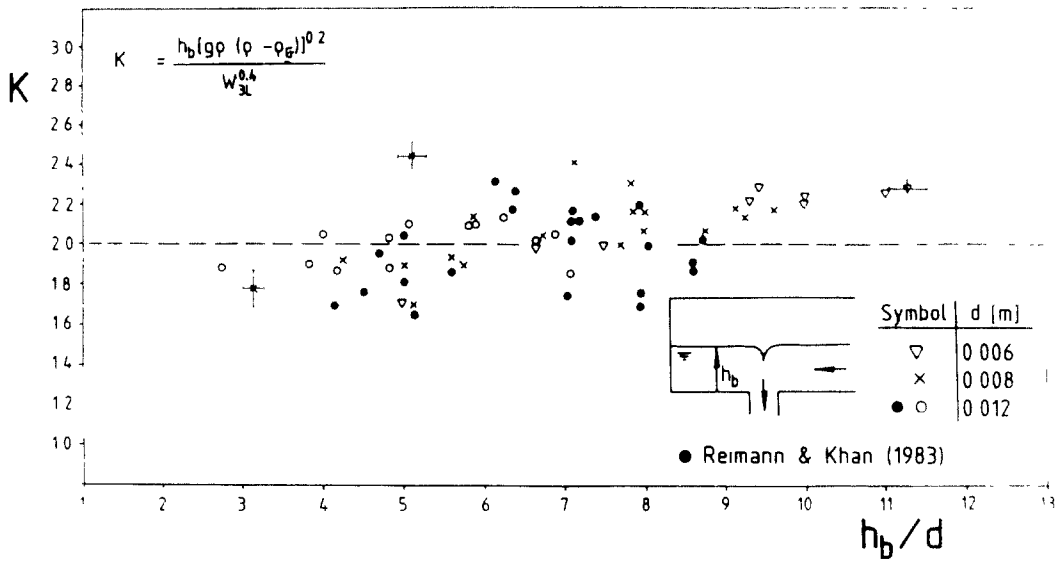

Figure 8 Beginning of gas entrainment in downward branch

1984). Equation [2] consequently, can be used to describe the b.e. in downward, upward and horizontal branches. Different values of K should be expected for different flow configurations.

For the b.e. in the three geometries investigated, the value of K given by [2] was plotted as a function of h_b/d. The data for b.g.e. in downward branches, with a vortex flow regime (figure 8) show good agreement with previous results (Reimann & Khan 1983). It is worth mentioning that for the transition from vortex to vortex-free flow in downward branches without superimposed velocities, the value $K = 0.69$ was obtained which coincides with the result for b.g.e. in the transient experiments from Lubin & Hurwitz (1966) in which a vortex-free flow was always observed. Data for b.l.e. in upward branches are presented in figure 9: The result $K = 1.67$ does not coincide with the value $K = 0.59$ obtained with the correlation proposed by Rouse *et al.* (1956). Data for b.l.e. and b.g.e. in horizontal branches are shown in figures 10a and 10b, respectively. The results in figure 10 show a discrepancy relative to the value $K = 0.15$ obtained by Gariel (1949), which could be

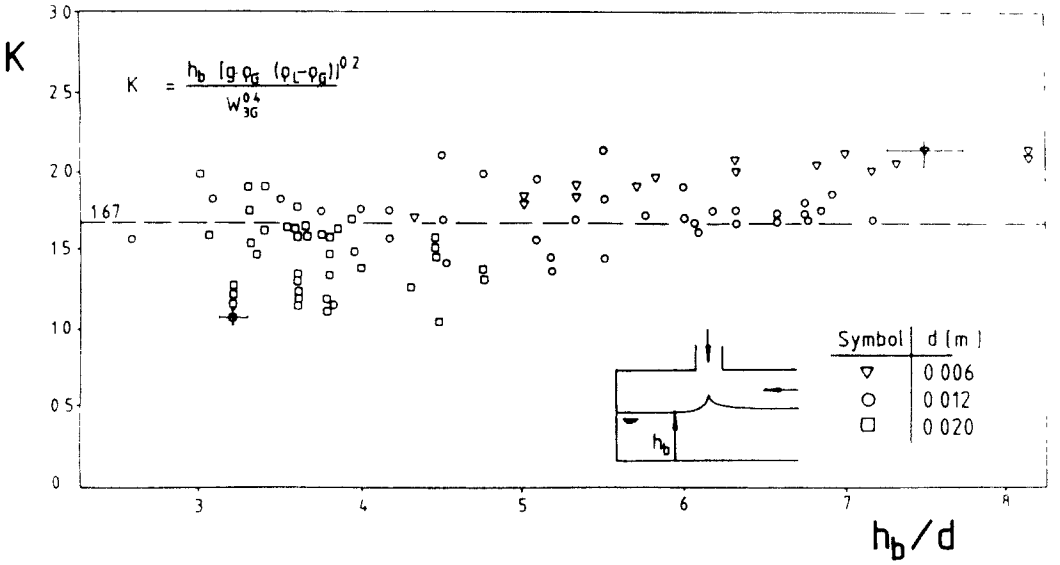

Figure 9 Beginning of liquid entrainment in upward branch

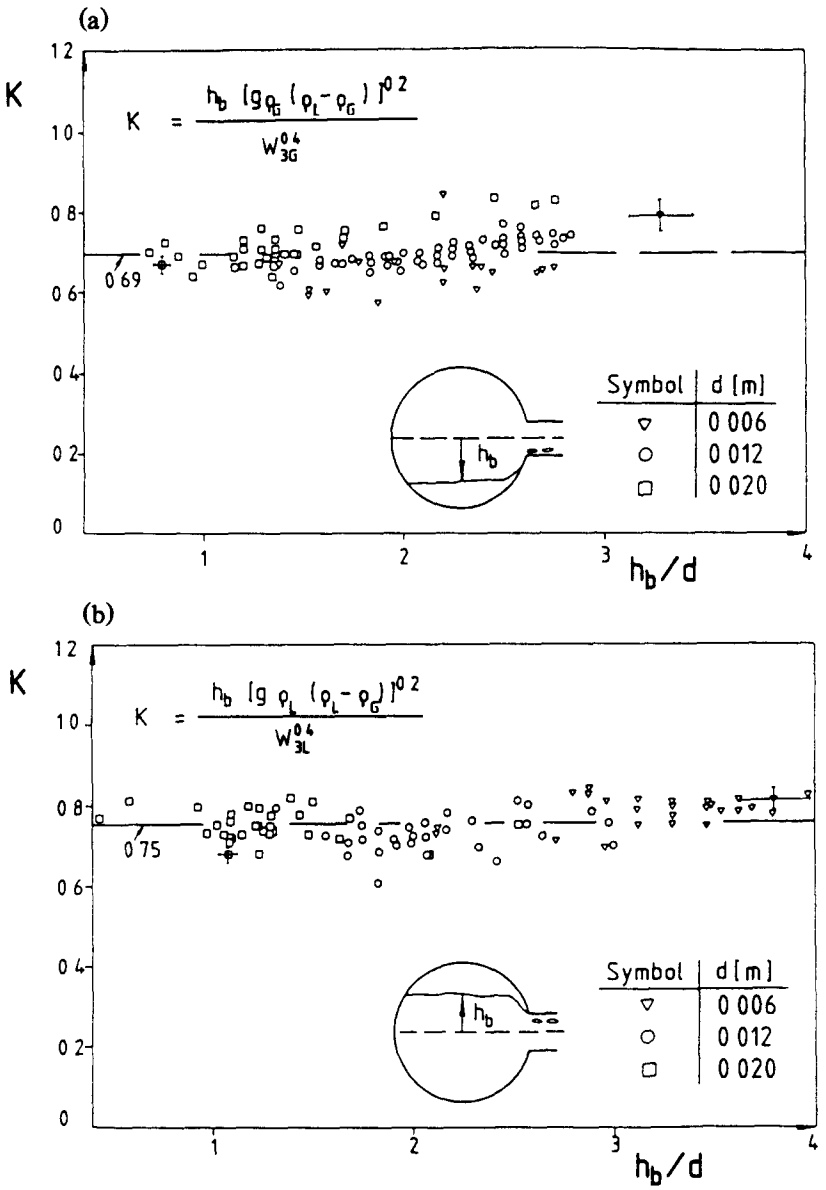

Figure 10. Beginning of entrainment in horizontal branch: (a) beginning of liquid entrainment; (b) beginning of gas entrainment.

attributed to differences in the flow field. For the different flow geometries no dependency of K on h_b/d is observed.

The data scatter in the general results follows from the characteristic fluctuations of the flow field described above.

Results with superimposed velocities are presented by Smoglie (1984): A significant influence was observed only for downward branches. Figure 11 shows the values of K for the b.g.e. in downward branches with $v_{2L} > 0$, as a function of the momentum flux $\rho_L v_{2L}^2 / \rho_b v_{3b}^2$. After the transition from vortex to vortex-free flow ($v_{2L} \geq 0.36$ m/s) a constant value of K different from that corresponding to vortex flow was obtained. For b.l.e. in upward branches, a slowly decreasing K was obtained for increasing v_{2G}, until slug flow occurred in the main pipe ($v_{2G} \approx 2.1$ m/s) which prevented reaching a possible transition to a vortex-free branch gas flow. Therefore a new constant value of K could not be obtained.

Results for b.g.e. ($v_{2L} < 0.5$ m/s) and b.l.e. ($v_{2G} < 1.6$ m/s) in horizontal branches show only a slight influence of the superimposed velocities on the values of K. From these results it follows that the values of K from figures 9 and 10 could be used together with

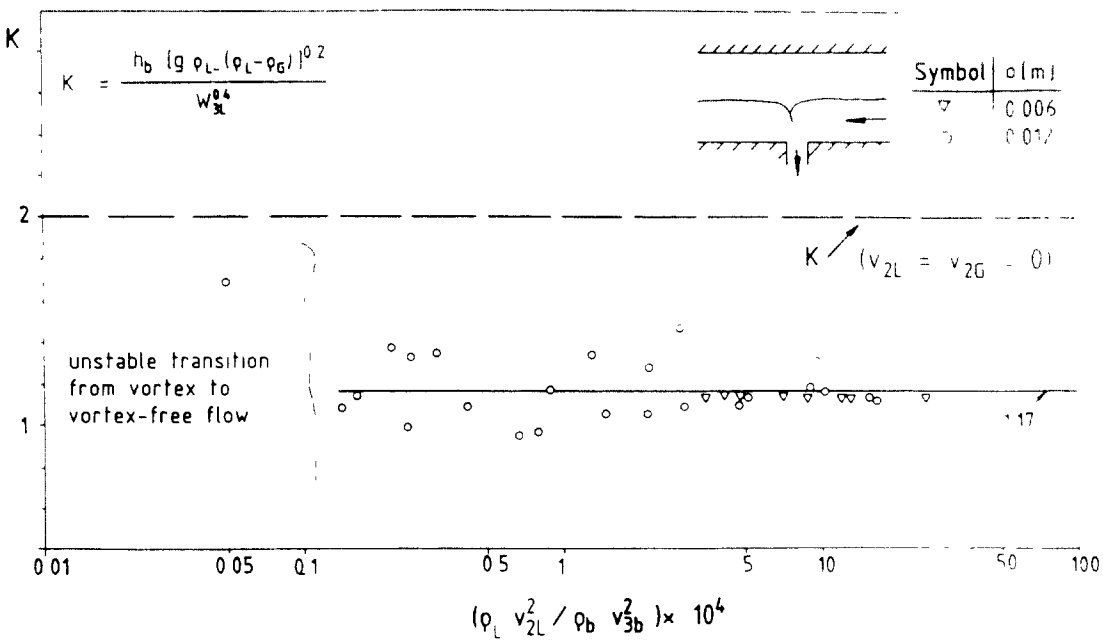

Figure 11. Beginning of gas entrainment in downward branch with superimposed liquid velocity $v_{2L} < 0.36$ m/s

[2] to determine the b.e. in small breaks at the top or on the side of large reservoirs, in which the small momentum of the fluid does not modify the value of K

5 GAS AND LIQUID ENTRAINMENT

5.1 Generalized representation of data

In the problem of small breaks in horizontal pipes, the determination of the branch quality x_3 and mass flux G_3 occurring during entrainment, i.e. when $h < h_b$, is of great importance.

To present the data for liquid or gas entrainment, the measured h and G_3 were normalized with the parameters h_b and G_{3b} respectively, which correspond to the b.e. calculated with the same system pressure P_1 and pressure difference ΔP_{1-3} measured during entrainment. The single-phase mass flux was determined by

$$G_{3b} = \zeta\epsilon\sqrt{\rho_b\,\Delta P_{1-3}} \qquad [3]$$

where ζ is the flow coefficient and ϵ the gas expansion coefficient.

The branch mass flow rate is given by

$$W_{3b} = \zeta\epsilon A_3\,\sqrt{\rho_b\,\Delta P_{1-3}} \qquad [4]$$

where A_3 is the branch cross-sectional area. Substituting [4] in [2], we obtain:

$$h_b = \frac{K(\zeta\epsilon A_3)^{0.4}}{g^{0.2}}\left(\frac{\Delta P_{1-3}}{\rho_L-\rho_G}\right)^{0.2} \qquad [5]$$

5.2 Branch quality

Horizontal branch. Figure 12 shows the normalized interface level in the range $-1 < h/h_b < 1$, as a function of the measured quality; reasonably good agreement with earlier data by Crowley & Rothe (1981) is observed. Data for different branch diameters

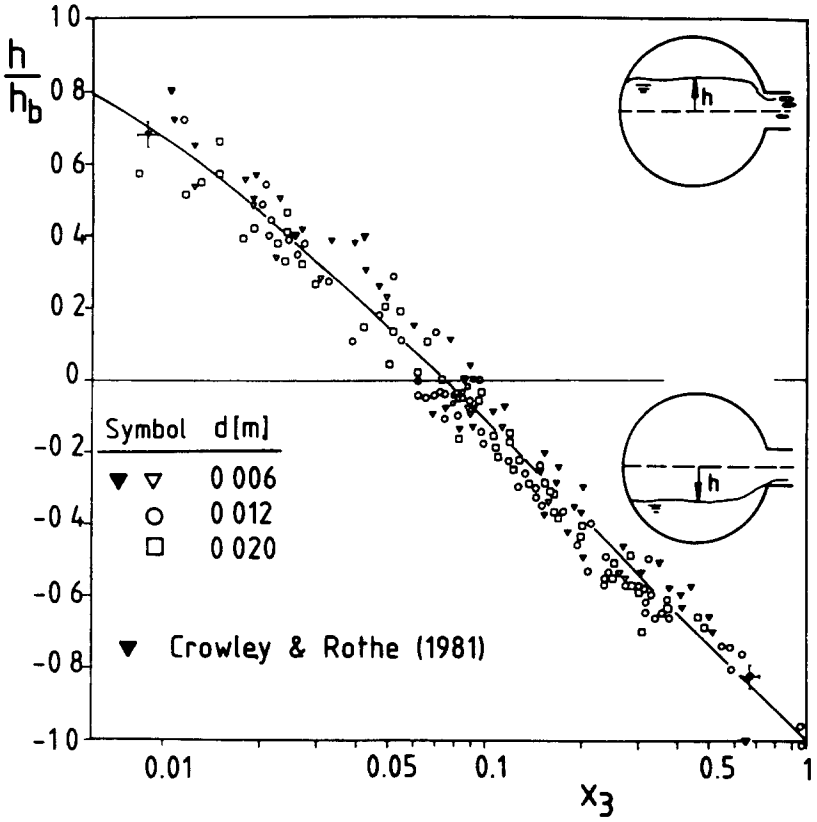

Figure 12. Quality in horizontal branch: gas and liquid entrainment.

d and pressure drops ΔP_{1-3} for both liquid and gas entrainment were fitted with a single relationship:

$$x_3 = x_0^{\left(1+C\frac{h}{h_b}\right)}\left[1 - \frac{1}{2}\frac{h}{h_b}\left(1+\frac{h}{h_b}\right)x_0^{\left(1-\frac{h}{h_b}\right)}\right]^{0.5} \qquad [6]$$

where x_0 represents the quality for $h = 0$.

The coefficient C accounts for the change in the parameter h_b when passing from liquid to gas entrainment (see [5]). For l.e. $(h/h_b \leq 0)$, $C = 1$ and for g.e. $(h/h_b \geq 0)$, $C = h_{bge}/h_{ble}$. Using [5] with $\epsilon_{air} = 0.96$ and the values of K from figure 10 results in $C = 1.09$.

To obtain a simple model for x_0, it was assumed that for $h = 0$, that means $\alpha = 0.5$, both phases have the same acceleration pressure drop:

$$\frac{1}{2}\rho_G v_{3G}^2 = \frac{1}{2}\rho v_{3L}^2 \qquad [7]$$

This assumption disregards the influence of superimposed flows parallel to the main pipe and pressure losses due to irreversible processes during the acceleration of the fluid.

Using [7] together with the definitions of mass flux and quality, we obtain:

$$x_0 = |1 + (\rho_L/\rho_G)^{0.5}|^{-1} \qquad [8]$$

To verify this expression, additional experiments were conducted at system pressures between 0.15 and 0.55 MPa. The measured x_0 values were about 15% higher than those given by [8]; the deviations were independent of P_1, ΔP_{1-3} and d. This discrepancy is not

surprising considering the complexity of the flow pattern in the vicinity of the branch entrance.

Thus, the final correlation proposed to predict the quality (x_{3pr}) in horizontal branches is:

$$x_{3pr} = \left[\frac{1.15}{1 + (\rho_L/\rho_G)^{0.5}}\right]^{\left(1+C\frac{h}{h_b}\right)} \left[1 - \frac{1}{2}\frac{h}{h_b}\left(1+\frac{h}{h_b}\right)\left(\frac{1.15}{1 + (\rho_L/\rho_G)^{0.5}}\right)^{\left(1-\frac{h}{h_b}\right)}\right]^{0.5} \quad [9]$$

where:

$$C = \begin{cases} 1 \text{ for l.e. } (h/h_b < 0) \\ 1.09 \text{ for g.e. } (h/h_b > 0) \end{cases}$$

Downward branch. Figure 13 shows results including earlier data (Reimann & Khan 1983). Different symbols are used to distinguish between experiments with superimposed velocities and those without. When h goes to zero, x_3 goes to unity; therefore, [9] was modified to satisfy this condition and the following relationship is proposed:

$$x_{3pr} = \left(\frac{1.15}{1 + (\rho_L/\rho_G)^{0.5}}\right)^{\left(2.5\frac{h}{h_b}\right)} \left[1 - \frac{1}{2}\frac{h}{h_b}\left(1 + \frac{h}{h_b}\right)\left(\frac{1.15}{1 + (\rho_L/\rho_G)^{0.5}}\right)^{\left(1-\frac{h}{h_b}\right)}\right]^{0.5} \quad [10]$$

where a value of 2.5 for the exponent resulted in a minimum mean square error.

Upward branch. Results for various flow regimes, including test points with critical branch flux, are presented in figure 14. For decreasing h/h_b the solid curve shows a relatively small change in x_3 until a sudden decrease occurs at $h/h_b \simeq 0.6$, which corresponds to the transition from stratified to slug flow in the main pipe.

The l.e. in an upward branch can be considered to be equivalent to the g.e. in a downward branch with gas and liquid being replaced by liquid and gas respectively:

$$x_{3pr}(\text{upward}) = 1 - x_{3pr}(\text{downward}) \quad [11]$$

where x_{3pr}(downward) is given by [10]. Considering again the change in the normalization factor h_b when passing from g.e. (downward) to l.e. (upward), the exponent 2.5 h/h_b used

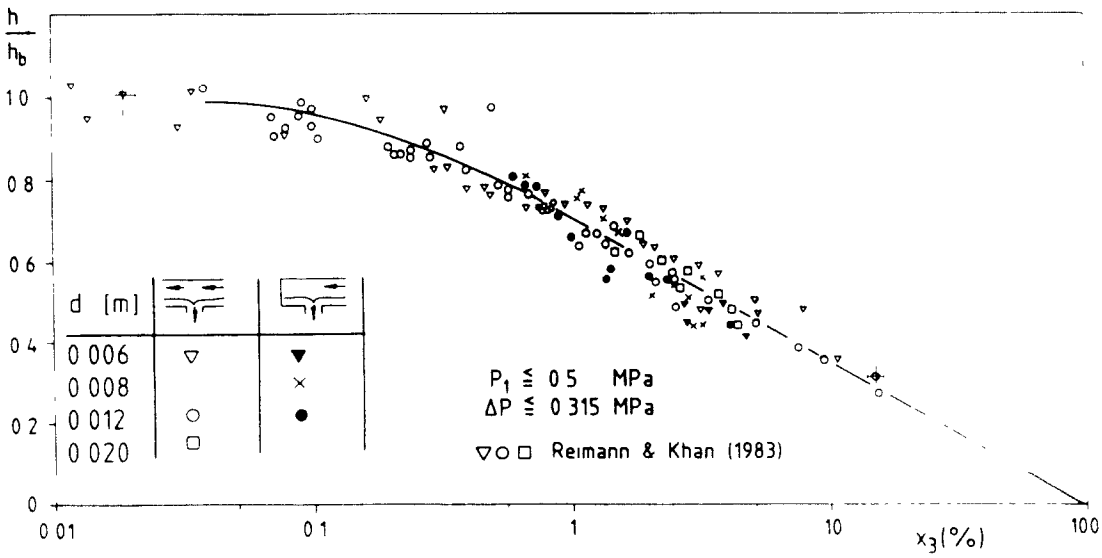

Figure 13 Quality in downward branch: gas entrainment

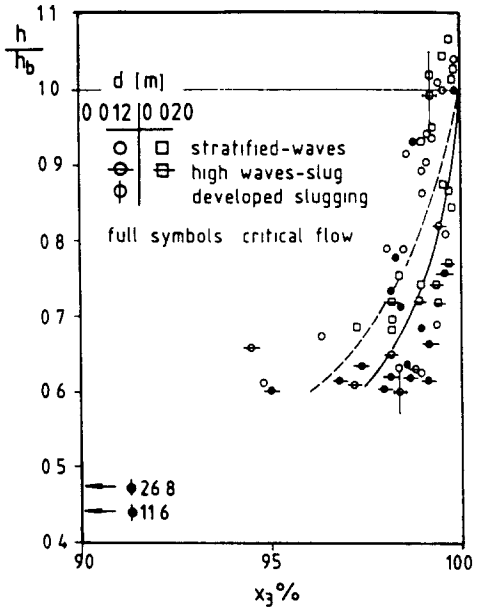

Figure 14. Quality in upward branch. liquid entrainment.

in [10] was multiplied by the correction factor $C_1 = 0.8$, thus, the expression proposed in [11] becomes:

$$x_{3pr} = 1 - \left(\frac{1.15}{1 + (\rho_L/\rho_G)^{0.5}}\right)^{\left(2\frac{h}{h_b}\right)} \left[1 - \frac{1}{2}\frac{h}{h_b}\left(1 + \frac{h}{h_b}\right)\left(\frac{1.15}{1 + (\rho_L/\rho_G)^{0.5}}\right)^{\left(1-\frac{h}{h_b}\right)}\right]^{0.5} \quad [12]$$

This correlation was used to plot the dashed curve in figure 14, assuming $P_1 = 4$ bar. The discrepancy relative to the mean value of the experimental results is small.

It should be noted that [9], [10] and [12] are functions of the density ratio and dimensionless interface level only. These correlations are believed to be applicable to arbitrary fluids and arbitrary flow geometries downstream of the branch entrance, i.e. they should be valid for orifices, pipe stubs, nozzles, etc.

For the three branch orientations the ratio of measured to predicted quality (x_3/x_{3pr}) was plotted as a function of h/h_b (Smoglie 1984). A fairly symmetric distribution about the value $x_3/x_{3pr} = 1$ was obtained for all geometries. Excluding the data for downward branches with $x_3 < 0.1\%$, where an error of $\pm 5\%$ in h/h_b can introduce an error greater than 100% in the predicted quality (see figure 13), standard deviations of 19, 30 and 1.5% were obtained for horizontal, downward and upward branches, respectively.

5.3 Branch mass flux

For g.e. and l.e. the normalized branch mass flux G_3/G_{3b} was plotted as a function of h/h_b. Again the experimental points were fitted by single curves. Figure 15 shows results for horizontal branches: the different values of G_{3b} for l.e. and g.e. (see [3]) are the reason for the discontinuity at $h = 0$. Again no remarkable differences are observed relative to earlier data by Crowley & Rothe (1981). Figure 16, for downward branches, again shows good agreement with earlier data. The qualities around 100% obtained for l.e. in upward branches (figure 14) determine the value $G_3/G_{3b} \simeq 1$ shown in figure 17. A strong increase in G_3/G_{3b} occurs as the slug flow regime is reached ($h/h_b \simeq 0.6$).

With an appropriate model giving G_3 as a function of x_3, the results in figures 15, 16 and 17 could be combined with [9], [10] and [12] to determine the total branch mass flux in horizontal, downward and upward branches, respectively. The models for the branch mass flux however are strongly dependent on the branch geometry and therefore will be different for orifices, nozzles, pipe studs, etc.

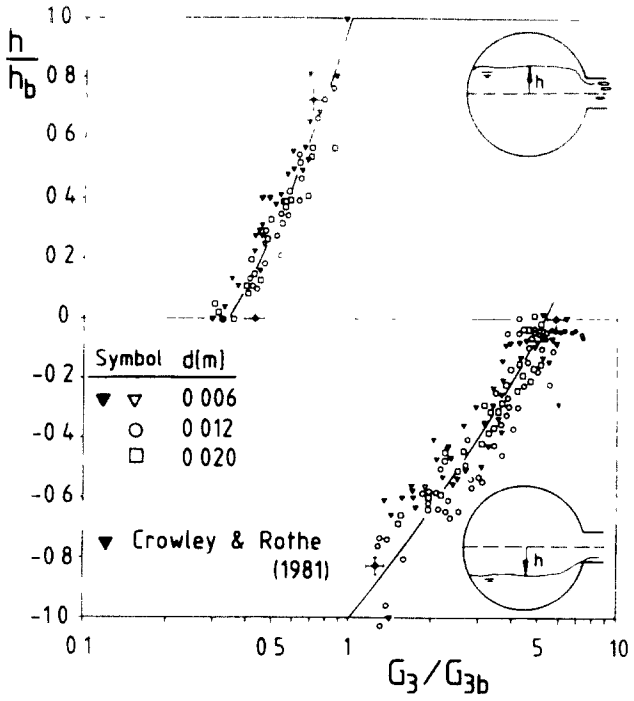

Figure 15 Mass flux in horizontal branch: gas and liquid entrainment

6 CRITICAL STEAM–WATER FLOW IN THE BRANCH

During a small break LOCA, a critical steam–water flow at high pressure occurs. Therefore, the above correlations must be combined with an appropriate model for the critical two-phase mass flow rate. Such models depend strongly on the break geometry (see e.g. Wallis 1980). It is not the purpose of this work to model in detail the present specific break geometry but rather to explain the procedure and highlight typical tendencies. The following assumptions are made: (a) the phases are ideally stratified; (b) there is no effect of the flashing, produced by the pressure drop in the vicinity of the break, on the flow field near the horizontal interface

As an example, the Homogeneous Equilibrium Model (HEM) is considered (compare, e.g. D'Auria & Vigni 1980) which determines the critical mass-flux in the break cross section as a function of the stagnation quality and stagnation temperature. Thus, for critical branch mass flux at a given system pressure P_1, the parameter h_b can be calculated using [2] with

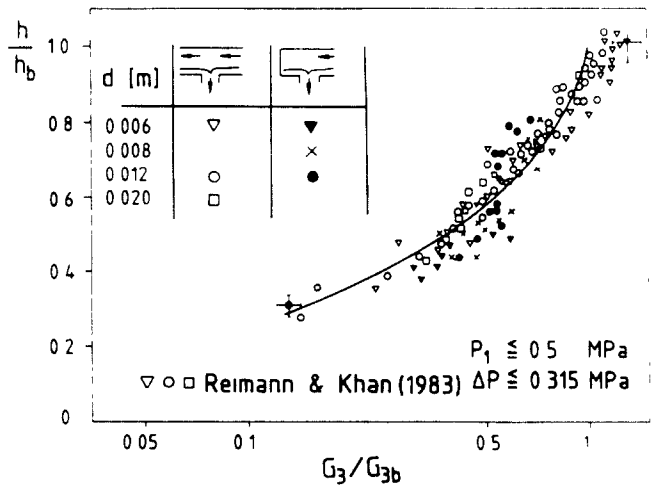

Figure 16 Mass flux in downward branch: gas entrainment

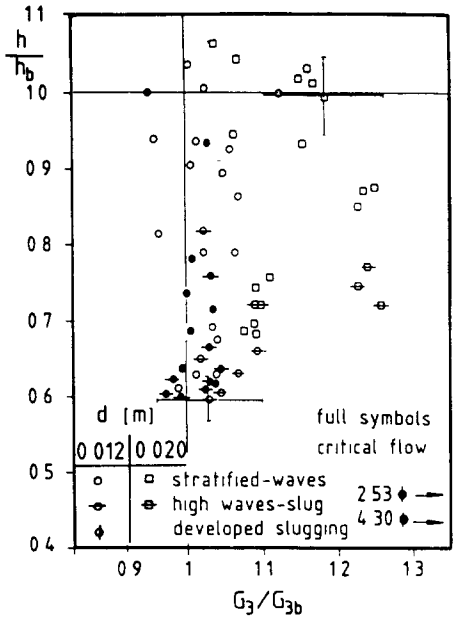

Figure 17. Mass flux in upward branch liquid entrainment.

W_{3b} as given by the HEM with $x_3 = 0$ for g.e. or $x_3 = 1$ for l.e. The hypothesis made to derive [8] concerns only the flow field upstream of the break. The model proposed for x_0 should be independent of the flow behavior downstream of the branch entrance (i.e. valid also for critical branch flow), and [9], [10] or [12] can be used to calculate the branch quality for arbitrary values of h and P_1. With this value of x_3 interpreted as the stagnation quality, again, as an example, the HEM can be used to determine the corresponding critical branch mass flux.

The procedure outlined above was applied to predict the steam–water branch mass flux G_3 and quality x_3 at a system pressure of 10 MPa through a side break ($d = 0.049$ m) in a horizontal coolant pipe ($D = 0.75$ m) which results in a ratio of break to main pipe cross-section of 0.4%, the rsults are shown in figure 18.

The present model is compared with two other models, presently used to describe the two-phase flow from a large pipe to a small break:

(a) The model used in the RELAP4 computer code (Katsma *et al.* 1976), which assumes that the branch inlet void fraction α_3 is equal to the upstream void fraction α_1:

$$\alpha_3 = \alpha_1 \qquad [13]$$

(b) The model used in the RELAP5 computer code (Ransom *et al.* 1981), where the void fraction α_3 is given by:

$$\alpha_3 = \alpha_1 \left(\frac{v_{1G}}{v_{GL}}\right)^{0.5} \quad \text{for } h_L > \frac{D+d}{2} \qquad [14]$$

$$\alpha_3 = 1 - (1 - \alpha_1)\left(\frac{v_{1G}}{v_{GL}}\right)^{0.5} \quad \text{for } h_L < \frac{D-d}{2} \qquad [15]$$

where v_{GL} is the gas velocity for the transition from stratified to slug flow as given by Taitel & Dukler (1978):

$$v_{GL} = \frac{h_G}{D}\left|\frac{(\rho_L - \rho_G) g A_G}{\rho_G A'_L}\right|^{0.5} \qquad [16]$$

where $A'_L = D[1-(2\,h_L/D-1)^2]^{0.5}$ and h_G is the gap of gas above the liquid.

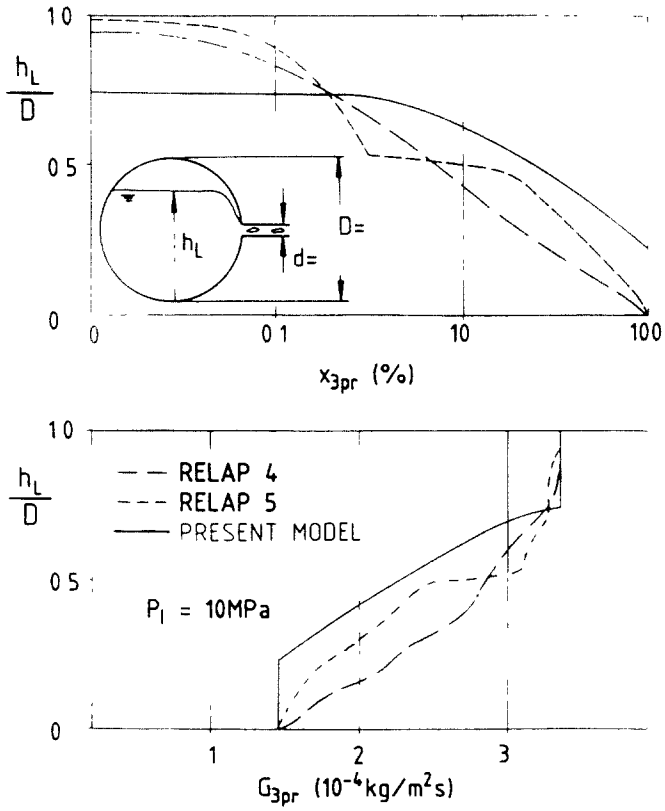

Figure 18 Quality and critical mass flux in horizontal branch

To determine the branch quality, again the HEM was used together with the void fractions given in [13] (RELAP4) or [16] (RELAP5) for $v_{1G} = 1$ m/s.

Figure 18 shows the comparison: the differences between the predicted qualities depend strongly on the liquid level. For h_L/D below the value corresponding to b.g.e., the qualities according to the present model are greater than those given by RELAP4 and RELAP5, the maximum difference being one order of magnitude.

The corresponding values for G_{3pr} show that for a wide range of h_L/D the mass fluxes calculated with the present model are lower than the values given by RELAP4 and RELAP5.

7 CONCLUSIONS

The flow through small breaks in horizontal pipes with stratified two-phase flow can be influenced considerably by gas or liquid entrainment as a consequence of the local pressure decrease produced by the acceleration of the fluid towards the break.

A vortex or a vortex-free flow occurs depending on the branch orientation and superimposed velocities.

From similitude between the flow fields generated by a small break and a point sink, a general correlation was obtained to determine the beginning of entrainment in upward, downward and horizontal branches.

A correlation is given to predict the branch quality for arbitrary fluid systems. Results corresponding to steam–water critical flow in horizontal branches show considerable discrepancy with values given by the computer codes RELAP4 and RELAP5.

To a certain degree the results are believed to be applicable to other geometries, e.g. to outlets at various positions in large reservoirs.

More theoretical work is desirable to model the entrainment processes in a more physically-based way. Further experiments with single-component fluids are necessary to investigate the influence of local flashing on the entrainment process.

Acknowledgements— The authors gratefully acknowledge the financial support given by the KfK and Centro Atomico Bariloche, Argentina and the stimulating discussions with Prof. Dr. U. Müller (KfK)

REFERENCES

AZZOPARDI, B. J. & WHALLEY, P. B. 1982 The effect of flow patterns on two-phase flow in a *T*-junction. *Int. J. Multiphase Flow* **8**, 491–507.

CRAYA, H. 1949 Theoretical research on the flow of non-homogeneous fluids. *La Houille Blanche*, 44–55.

CROWLEY, C. J. & ROTHE, P. H. 1981 Flow visualization and break mass flow measurements in small break separate effects experiments. *ANS Specialist Meeting on Small Break Loss of Coolant Accident Analyses in LWR's*, Monterey, California, 25–27 August.

DAGGET, L. & KEULEGAN, G. 1974 Similitude in free surface vortex formation. *J. Hydr. Div. ASCE,* **100**, 1506.

D'AURIA, F. & VIGNI, P. 1980 Two-phase critical flow models, CSNI Report No. 49.

GARIEL, P. 1949 Experimental research on the flow of non-homogeneous fluids. *La Houille Blanche*, 56–64.

HENRY, J. A. R. 1981 Dividing annular flow in a horizontal tee. *Int. J. Multiphase Flow* 7, 343–355

JOHN, H. & REIMANN, J. 1979 Gemeinsamer Versuchsstand zum Testen und Kalibrieren verschiedener Zweiphasen-Massenstrom-Messverfahren. KfK 2731 B.

KATSMA, K. R., FISCHER, S. R., NELSON, R. A., BARNUM, D. J., JAYNE, G. A., JOHNSEN, G. W., YOUNG, R. C., CURTIS, R. L., WAGNER, R. J., WELLS, R. A., SINGER, G. L., TOLLI, J. E., BURGESS, C. J., NOBLE, C., RETTIG, W. H. 1976 *User's Manual for RELAP4/MOD.5.* INEL-Report, ANCR-NUREG-1335.

LUBIN B. & HURWITZ, M. 1966 Vapor pull-through at a tank drain with and without dielectrophoretic buffling. *Proc. Conf. Long Term Cryopropellant Storage in Space,* NASA Marshall Space Center, Huntsville, Ala., 173.

RANSOM, V. H., WAGNER, R. J., TRAPP, J. A., CARLSON, K. E., KISER, D. M., KUO, H. H., CHOW, H., NELSON, R. A. & JAMES, S. W. 1981 *RELAP5/MOD1 Code Manual Vol.1: System Models and Numerical Methods.* NUREG/CR-1826 EGG-2070 DRAFT Revision 1.

REIMANN, J. & KHAN, M. 1983 Flow through a small pipe at the bottom of a large pipe with stratified flow. *Second Int. Topical Meeting on Nuclear Reactor Thermal-Hydraulics,* Santa Barbara, California, 11–14 January.

REIMANN, J. & SMOGLIE, C. 1983 Flow through a small pipe at the top of a large pipe with stratified flow. *Annual Meeting of the European Two-Phase Flow Group,* Zürich, Switzerland, 14–16 June.

ROUSE, H., DAVIDIAN, J., GLOVER, J. E. & APPEL, D. W. 1956 Development of the non-circulatory waterspont. *J. Hydraulics Division,* HY4, Paper 1038.

SABA, N. & LAHEY, R., JR. 1984 The analysis of phase separation phenomena in branching conduits. *Int. J. Multiphase Flow* **10**, 1–20.

SEEGER, W., REIMANN, J. & MÜLLER, U. 1985 Phase separation in the *T*-junction with a horizontal inlet. *2nd International Conference on Multi-Phase Flow.* London, England, 19–21 June.

SMOGLIE, C. 1984 Two phase flow through small branches in a horizontal pipe with stratified flow. KfK 3861.

SMOGLIE, C. & REIMANN, J. 1984 Two-phase flow through a small horizontal branch in a pipe with stratified flow. *Jahrestagung Kerntechnik '84,* Frankfurt 22–24 Mai.

TAITEL, Y. & DUKLER, A. E. 1978 Transient gas–liquid flow in horizontal pipes: modeling the flow pattern transitions *AIChE J.* **24**, 920–934.

WALLIS, G. B. 1980 Critical two-phase flow. *Int. J. Multiphase Flow* **6**, 97–112.

ZUBER, N. 1981 Problems in modeling of small break LOCA. NUREG-0724.